Innovative Elastomer Transducer Driven by Karman Vortices in Water Flow

Seiki Chiba[1], Kenta Hasegawa[2], Mikio Waki[3], Koji Fujita[4], Kazuhiro Ohyama[5] and Shijie Zhu[5]

1. Chiba Science Institute, 3-8-18 Yakumo, Meguro-Ward, Tokyo 152-0023, Japan

2. National Maritime Research Institute, 6-38-1 Shinkawa, Mitaka-City, Tokyo 181-0004, Japan

3. Wits Inc., 880-3 Oshiage, Sakura-City, Tochigi 329-1334, Japan

4. Institute of Space and Astronautical Science, Japan Aerospace Exploration Agency, Sagamihara City, Kanagawa 252-5210, Japan

5. Fukuoka Institute of Technology, Fukuoka-City, Fukuoka 811-0295, Japan

Abstract: A simple experimental model of a power generation system was tested in a flowing water tank in order to investigate the performance and feasibility of a small hydroelectric generation system using DE (dielectric elastomer) transducer. The mass of DE material in the power generator module was only 0.1 g. The electric energy generated with a stroke of 10 mm was 12.54 mJ. An electrical energy of approximately 1.5 J per cycle of DE generators can be expected to be generated by scaling up this system, which is capable of being equipped with up to about 100 units of DE transducers. The water velocity was set at 0.30 to 0.70 m/s. This is a small flow, about the same flow as the water in a Japanese garden. This system was driven by Karman vortices in the wake of a cylinder fixed in the water flow. The characteristics of DEs can be utilized to produce electric power effectively. A wing, which is an important part in the generation system to convert fluid energy into mechanical energy, was set behind the cylinder. The wing oscillated due to the pressure caused by Karman vortices, resulting in stretching and contracting of the DE transducers, thus producing electrical power. Experimental results show that an average output power of approximately 31 mW was produced with a generation efficiency of about 66%, when the diameter of the cylinder is 60 mm, the span and chord length of the wing are 120 mm and 30 mm, respectively, the distance between the cylinder and the wing is 170 mm, and the velocity of the water flow is 0.50 m/s.

Key words: Artificial muscle, actuator, DE, hydro power generation, wing power generation, Karman vortex.

1. Introduction

Almost all commercial electric generation uses electromagnetic induction, in which an electric generator rotates due to mechanical energy. The mechanical energy can be produced by a turbine driven by wind, falling water or flow from a stream, for example. Today there is a great hope that small-scale power generation utilizing renewable energy sources will come into wide use as problems from environmental pollution and population increase [1]. Conventional electric generators using electromagnetic induction, however, may not be suitable for renewable energy sources, because they tend to operate most efficiently over a narrow range of high frequencies [2]. Renewable energy sources usually produce motions over a wide range of lower frequencies, and accordingly, electricity generation systems using electromagnetic induction must include a mechanical or hydraulic transmission, resulting in systems that are more complex and expensive. DE (dielectric elastomer) is one of the most promising artificial muscles, and a new transducer technology that is capable of converting mechanical energy into electrical energy. Compared to conventional power generators using electromagnetic induction or the piezoelectric effect, generators using DEs have high energy density and can efficiently produce electricity at low frequency [3-6].

Although there are many studies on the VIV (vortex induced vibration) mechanism for small-scale power

Corresponding author: Seiki Chiba, Ph.D., CEO, research field: dieleastic elastomers.

generation with a simple structure, no other attempt has been made to apply DE to hydropower systems using VIV. Allen and Smits [7] examined the feasibility of placing a piezoelectric membrane in the wake of a bluff body and using Karman vortex street forming behind the bluff body to induce oscillations in the membrane. The vibration results in a capacitive buildup in the membrane that provides a voltage source that is capable of trickle-charging a battery in a remote location. Zhu et al. [8] reported a novel cantilever-based electromagnetic wind generator for a wireless sensing application. The generator consists of a bluff body, a magnet, a coil, and an airfoil attached to a cantilever spring. The airflow over the airfoil causes the oscillating motion of the cantilever, resulting in the degree of bending being a function of the lift force from the airfoil and the spring constant. The permanent magnet is fixed on the airfoil and the coil is attached to the device. The motion of the airfoil causes the magnetic flux cutting the coil to change, which generates electrical power. The device has dimensions of 12 cm × 8 cm × 6.5 cm. Experimental results show that the device can operate at wind speeds as low as 2.5 m/s with a corresponding electrical output power of 470 μW, which means it is sufficient for periodic sensing and wireless transmission. When the wind speed is 5 m/s, the output power is 1.6 mW. Akaydin et al. [9] evaluated the power generating performance of piezoelectric beams placed in the wake of a circular cylinder at high *Re* (Reynolds numbers) of 10,000 to 21,000. The beam has dimensions of 30 mm × 16 mm × 0.2 mm, and the cylinder has a diameter of 0.03 m and a length of 1.22 m. The experiments were carried out in a wind tunnel. The maximum output power of about 4 μW was obtained at Re = 14,800 in the device. Wang et al. [10] proposed a new electromagnetic energy harvester for harnessing energy from vibration induced by Karman vortex street. The variation of the liquid pressure in the wake of a bluff body drives a flexible diaphragm with an attached permanent magnet into

vibration. The vibration energy is converted to electrical energy by electromagnetic induction. They fabricated and tested a prototype of the energy harvester having a volume of 37.9 cm^3. Experimental results show that an instantaneous power of 1.77 μW is generated under a pressure fluctuation frequency of 62 Hz and a pressure amplitude of 0.3 kPa in the Karman vortex street. Wang et al. [11] also developed a new miniature hydro-energy generator using a cantilevered piezoelectric beam for harnessing energy from Karman vortex street behind a bluff body in a water flow. This system is capable of producing an output power of 0.7 nW when the pressure oscillates with an amplitude of nearly 0.3 kPa and a frequency of about 52 Hz. Nguyen et al. [12] presented a miniature pneumatic energy generator for harnessing energy from the Karman vortex street behind the bluff bodies in a tandem arrangement to enhance the amplitude of the pressure fluctuation in the vortex street, which vibrates a piezoelectric film. Experimental results show that the average output power is 0.59 nW, with a pressure oscillation amplitude of about 70 Pa and a frequency of nearly 872 Hz. Demori et al. [13] proposed an innovative energy harvesting system based on a piezoelectric converter to extract energy from airflow for autonomous sensors. The vibration of the blade induced by the Karman vortex street results in power being generated by the converter. Experimental results show that a harvested power of about 100 μW with retransmission intervals below 2 min is obtained.

In this study, we devised a new kind of small-scale power generation using a DE as an electric generator driven by Karman vortices in water flow. The energy of Karman vortices in a water flow can be converted to electric energy by a small diaphragm-type power generator using a DE. This system can be expected to perform effective power generation with a simple structure. In order to investigate its performance and feasibility, the system was fabricated and tested.

2. Background on DE Artificial Muscle

DE is a new transducer technology that has been under development since 1991 [14]. DE uses rubberlike polymers (elastomers) as actuator materials [15]. The basic element of DE is a very simple structure comprised of a thin elastomer sandwiched between compliant electrodes. When a voltage difference is applied between the electrodes, they are attracted to each other by electrostatic forces (Coulomb forces) leading to a thickness-wise contraction and plane-wise expansion of the elastomer. This deformation of the polymer can be used for actuation. The DE film can be made using several well-known techniques including spin coating, dip coating and casting [16].

Recently, the use of DE actuator in the reverse mode, in which deformation of the elastomer by external mechanical work is used to generate electrical energy, has been gaining more attention [17, 18]. Two approaches, (1) DE materials and mechanical systems using DEs [6, 19, 20, 21, 22, 23-27], and (2) operating strategies (circuit designs) [21, 28-30] are being studied at the present.

2.1 DE Generators

The operation principle in the generator mode is the transformation of mechanical energy into electric energy by deformation of the DE. Functionally, this mode resembles piezoelectricity, but its power generation mechanism is fundamentally different. With DE, electric power can be generated even by a slow change in the shape of DE [27], while for piezoelectric devices impulsive mechanical forces are needed to generate the electric power [31]. Also, the amount of electric energy generated and conversion efficiency from mechanical to electrical energy can be greater than that from piezoelectricity [31-34]. Fig. 1 shows the operating principal of DE power generation.

Application of mechanical energy to a DE membrane to stretch it causes a decrease in thickness and expansion of the surface area. At this moment, a voltage is applied to the membrane. The applied electrical energy is stored on the membrane as electric charge. When the mechanical energy decreases, the elastic recovery force of the film acts to restore the original thickness and to decrease the in-place area. At this time, the electric charge is pushed out the electrode direction. This change in the location of the electric charge increases the voltage difference, resulting in an increase of electrostatic energy.

$$C = \varepsilon_0 \varepsilon A / t = \varepsilon_0 \varepsilon b / t^2 \quad (1)$$

where ε_0 is the dielectric permittivity of free space, ε is the dielectric constant of the polymer film, A is the active polymer area, and t and b are the thickness and the volume of the polymer. The second equality in Eq. (1) can be written because the volume of elastomer is essentially constant, i.e., $At = b$ = constant.

The energy output of a DE generator per cycle of stretching and contraction is

$$E = 0.5 C_1 V_b^2 \left(C_1 / C_2 - 1 \right) \quad (2)$$

where C_1 and C_2 are the total capacitances of the DE films in the stretched and contracted states, respectively, and V_b is the bias voltage.

Considering then changes with respect to voltages, the electric charge Q on a DE film can be considered to be constant over a short period of time and in the basic circuit. Since $V = Q/C$, the voltages in the stretched state and the contracted state can be expressed as V_1 and V_2, respectively, and the following equation is obtained.

$$V_2 = Q/C_2 = \left(C_1 / C_2 \right)\left(Q/C_1 \right) = \left(C_1 / C_2 \right) V_1 \quad (3)$$

Since $C_2 < C_1$, the contracted voltage is higher than the stretched voltage, corresponding to the energy argument noted above. The higher voltage can be measured and compared with predictions based on this
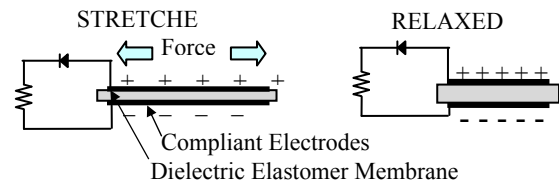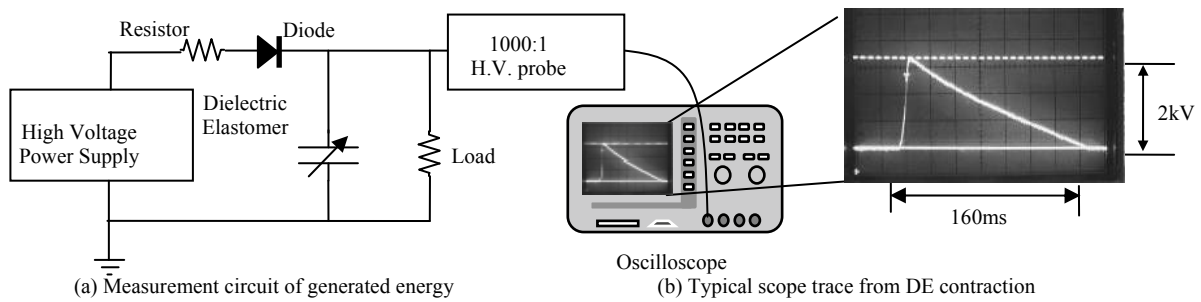

Fig. 1   Operating principle of DE power generation.

(a) Measurement circuit of generated energy   (b) Typical scope trace from DE contraction

Fig. 2   Voltage for DE compression and the measurement circuit: (a) Measurement circuit of generated energy, (b) Typical scope trace from DE contraction. Voltage spike occurs at contraction and gradually goes back to (stretched) voltage due to load resistance.

DE theory. In general, experimental data based on high impedance measurements are in excellent agreement with predictions [35]. When the conductivity is assumed to be preserved in the range of electric charging, Q remains constant.

Fig. 2a shows a simplified circuit for oscilloscope measurements of voltage, and Fig. 2b shows a typical scope trace from DE contraction.

*2.2 Recent Experiments of Wave Power Generators Using DEs*

In August 2007 in Tampa Bay, Florida, USA, we carried out the world's first marine experiment into power generation by natural sea waves using a DE power generator [32]. The total mass of DE material in the generators was 150 g. The maximum measured electrical output capacity, verified in laboratory tests, was 12 J per stroke for the generator. This system was designed to produce 12 J from an ocean wave having a wave height of 60 cm at bias voltage of 2,100 V. However, wave activity was minimal during the test period. Wave heights were on the order of few centimeters, which made it very difficult to carry out tests for wave-powered generators. On occasion the weather generated waves 10 cm high. Even with a wave height of 10 cm, we were able to generate a peak energy of 3.6 J at a bias voltage of 2,000 V (see Fig. 3). The generator uses a proof-mass to provide the mechanical forces that stretch and contract the DE generator, as shown in Fig. 3.

In December 2008, oceanic tests were also carried out in California, USA, and it was confirmed that generated electric energy was stored in a battery [36].

In November 2010, a new system that can generate electric energy from the fairly small amplitude waves which occur near shore protection was developed and tested for the first time. These marine tests for DEG were carried out using a fairly small buoy of 90 cm in diameter at Suzaki Port in Izu Peninsula (which is located 200 km south-west of Tokyo) [37]. The power generation buoy was moored by a wire in a water depth of 2.8 m using mooring equipment set on the shore protection wall (Fig. 4). The power generation module was set between the buoy and wire, so that the DE could be directly stretched by the up-down motions of the buoy due to waves.

The DE for the power generation module in this experiment weighed approximately 4.6 g, and was a cylindrical roll (26 cm in diameter and 12 cm in height)
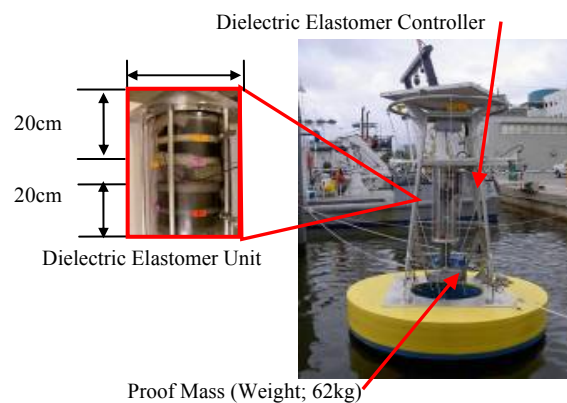
Fig. 3   DEG (dielectric elastomer generator) system on the buoy, having height of 7 m, used in December 2007.
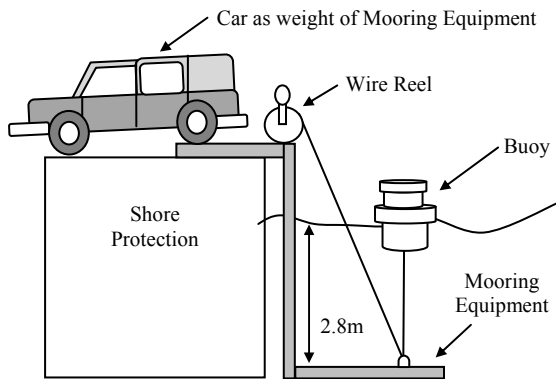
Fig. 4   The power generation buoy moored by a wire in a water depth of 2.8 m using mooring equipment set on the shore protection.
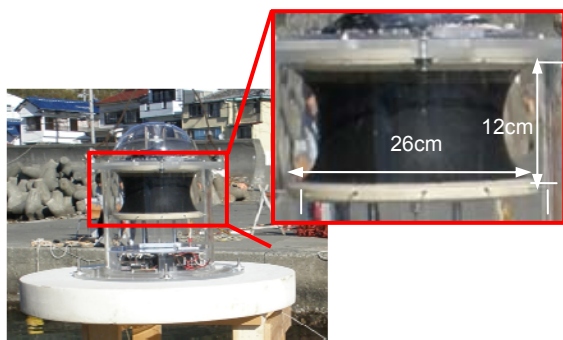
Fig. 5   The cylindrical roll DE power generation module, 26 cm in diameter and 12 cm in height, used in November 2010.

shown in Fig. 5. When a voltage of 3,000 V was applied to the DE, its maximum power generation was approximately 274 mJ each cycle from 6 cm stretched to relaxed states.

In this experiment, as the height of continuously occurring waves was approximately 14 cm, the electric power generated by each wave was about 131 mJ. At this time, the applied bias voltage was 2,100 V, and thus for 3,000 V at the same condition, the electric power generated is estimated to be about 274 mJ. Fig. 6 shows total electric power generation during 50 minutes in the case of a bias voltage of 2,100 V and 3,000 V. Fig. 7 shows total electric power generation vs. total DE stroke.

Recently, Moretti et al. [38], Vertechy et al. [39], and Chiba et al. [40] also showed that one of the most promising applications for DEGs was in the field of wave energy harvesting.

3. Experimental Details

A new device for small hydroelectric power generation system is based on a diaphragm type DEG. It is driven by a Karman vortex street in a water flow. The experimental details are as follows.

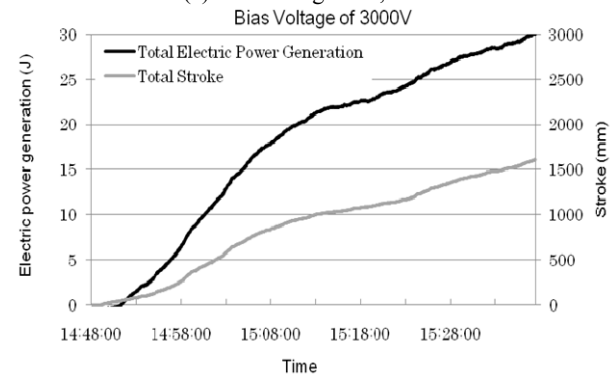### 3.1 Power Measuring Method for a Diaphragm Type DE Cartridge

The mass of the DE material in the module in this experiment is only 0.1 g. This active polymer is made
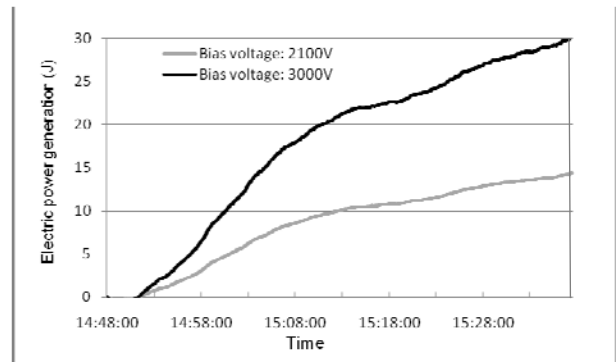
Fig. 6   Total electric power generation during 50 minutes in the case of bias voltage of 2,100 V and 3,000 V.
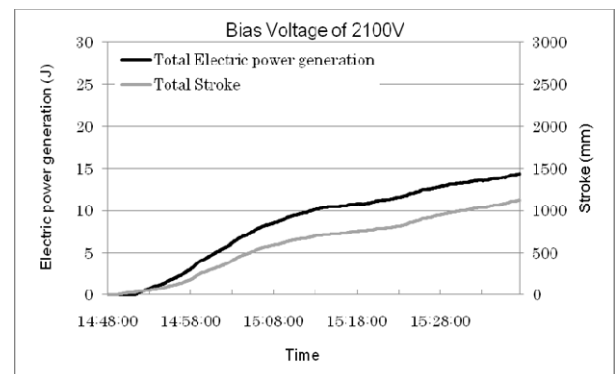
(a) Bias voltage of 2,100 V

(b) Bias voltage of 3,000 V

Fig. 7   Total electric power generation vs. total DE stroke.

from acrylic polymer (3M Corp., VHB4910). The electrode was based on carbon black with a polymer binder [34]. The electrodes were made by mixing carbon black and a polymer binder (silicon adhesive) and dipping into this solution. The average size of the carbon black was 50 nm. The average thickness of the polymer is 500 μm. The average thickness of the electrode is 15-20 μm. It was prestretched slightly to be diaphragm-shaped (80 mm in diameter and 1.4 mm in height: see Fig. 8). When a voltage of 2,800 V was applied to the artificial muscle, its maximum power generation was approximately 12.54 mJ. The stroke from stretched to relaxed states was 10 mm.

The electric power (E) obtained by the generator was estimated by the following method:

(1) The relation $C_1 = V_2C_2/V_1$ is derived from Eq. (2), and then by introducing C_1 into Eq. (2), the electric power generated is obtained.

$$E = 0.5V_1V_2C_2(V_2/V_1 - 1) \qquad (4)$$

(2) Using Eq. (4) and the values of C_2 and V_2, the generated electric power can be determined.

(3) The values of C_2 and V_2 were obtained as follows.

• The voltage (V_2) between the electrodes on both surfaces of the DE in the contracted state was measured at each cycle period as shown in Fig. 9 [35].

• The capacitance (C_2) of the DE at the contracted state was also measured at each wave period as shown in Fig. 10 [35].

The generating capacity for each stroke was measured with a unit DE cartridge (see Fig. 11a). An electric power of 12.54 mJ was obtained by Eq. (4) and the measured values of C_2 and V_2 at a stroke of 10 mm. Fig. 11d shows the relation between the stroke and the electrical energy. The relationship appears to be linear.

The stroke and the external force which gives a stroke to DE, shown in Fig. 11c, appear to also be linearly related. Therefore, the external force and the electrical energy exhibit linearity as well. The electric energy generated with a stroke of 10 mm is 12.54 mJ.

An external force of 4.05 N is required. This DE component can be considered as a spring having a spring constant of 405 N/m.

3.2 Power Generation Principle Using Karman Vortex Street

The Karman vortex street is a series of vortices shed periodically in the wake of a bluff body (Fig. 12). The vortices are formed alternately on each side of the body and have opposite directions of rotation. These vortices do not mix with the outer flow and are dissipated by viscosity only after a long time. The
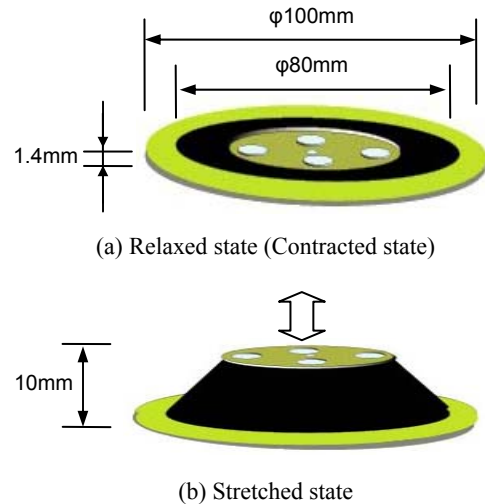

(a) Relaxed state (Contracted state)

(b) Stretched state

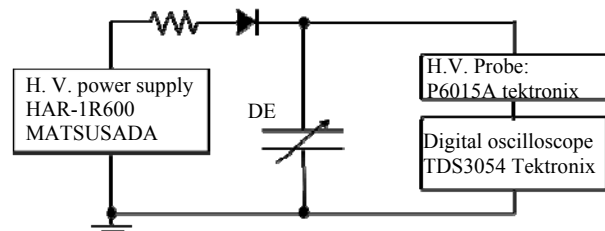**Fig. 8   Diaphragm-type, single layered DE artificial muscle (transducer) .**

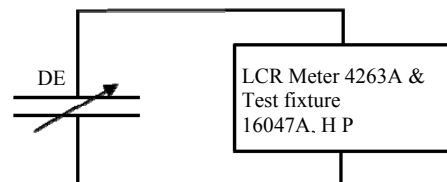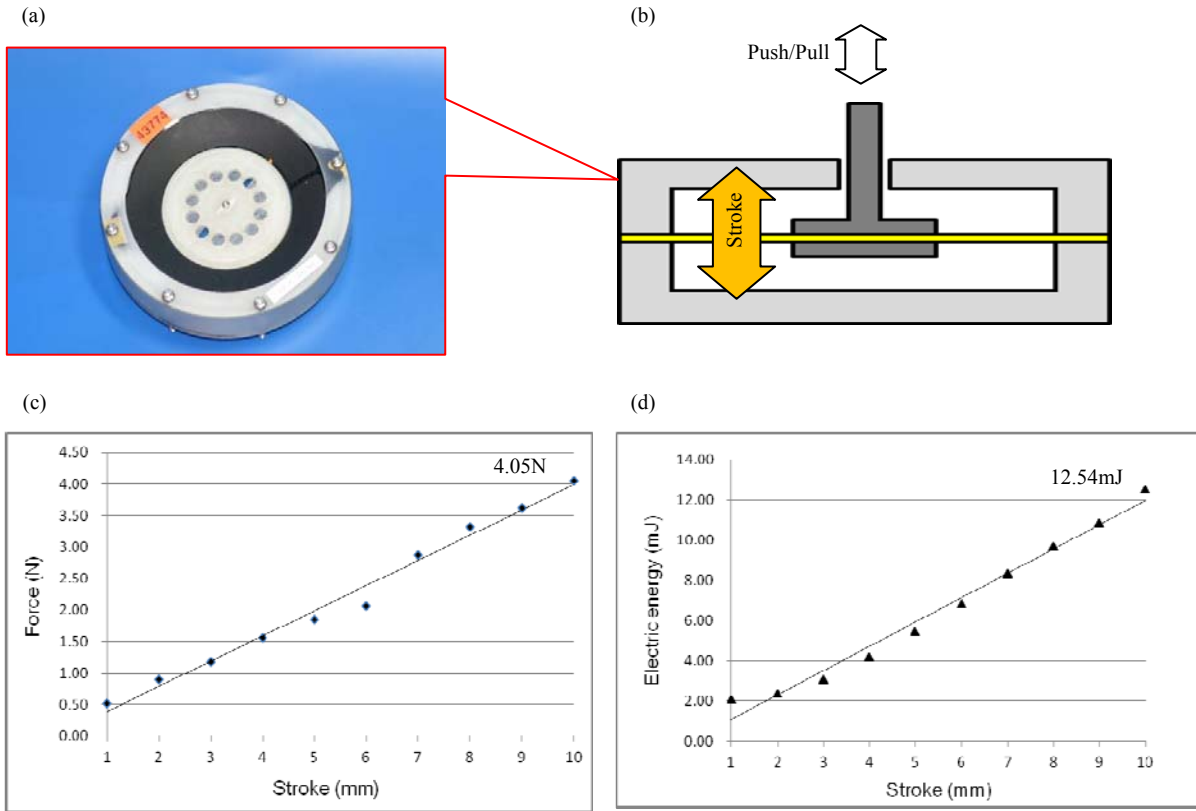**Fig. 9   Measurement circuit of a voltage of DE at a contracted state.**

Fig. 10   Measurement circuit of a capacitance of DE at a contracted state.

Fig. 11   (a) Photo of DE generator. The black part is DE with a diameter of 80 mm. The center of the device is pushed and released to function. (b) Cross section view of DE generator. DE film is set in the middle of the case. (c) Pushing force as a function of stroke. (d) Generated electric energy as a function of stroke.

Fig. 12   Image diagram of Karman vortex street.

Karman vortex street behind a cylinder occurs at Re from about 40 to 3.7×10^5 [41]. Re is a dimensionless value that measures the ratio of inertial forces to viscous forces and may be defined as:

$$Re = UD/v \qquad (5)$$

where U is the steady velocity of the flow upstream of the cylinder, D is the diameter of the cylinder, and v is the kinematic viscosity of the fluid. The frequency at which vortices are shed behind a cylinder in a Karman vortex street is related to the St (Strouhal number) by the following equation.

$$St = f_v D/U \qquad (6)$$

where f_v is the vortex shedding frequency. St is experimentally found to be approximately equal to 0.2 in $500 < Re < 3.7\times10^5$ [41] for circular cylinders.

On the basis of this phenomenon, a small hydroelectric generation system was designed. The system and the operation principles are illustrated in Fig. 13. Fig. 13a shows the top view of this system. A wing and two DEGs are set behind and ahead a cylinder respectively, connected by a shaft through a fulcrum. The cylinder is fixed in the uniform water flow, following Karman vortices. The wing vibrates, are attracted by the low pressure in the vortex, resulting in a stroke of the DEs (Fig. 13b).

3.3 Experimental Set-up

In order to experimentally verify the feasibility and estimate the power generation performance of the proposed hydroelectric power generation system, the
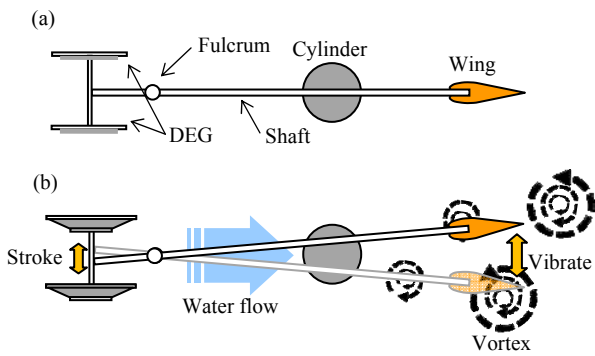
**Fig. 13   Schematic diagrams of the system and operation principles.**

model was fabricated and then tested in a two-dimensional circulating water channel that was 1,000 mm in length, 300 mm in width and with a water depth of 200 mm. Water velocity (U) was set at 0.30 to 0.70 m/s by 0.05 m/s increments. These velocities correspond to approximately $1.4 \times 10^4 < Re < 5.3 \times 10^4$ by Eq. (5). Fig. 14 shows a schematic drawing and a photo of the experimental apparatus, which is fixed on the water channel cover. Three kinds of cylinders made of polyvinyl chloride, which are fixed to the cover, were employed as bluff bodies to make a Karman vortex street. The height of the cylinders was 290 mm and the diameters (D) were 48, 60 and 76 mm. The two DEGs were located 470 mm ahead of the cylinder. A shaft made of aluminum is put between the DEGs. The DEs are deformed due to the movement of a wing, which is located in the region where the Karman vortices are formed. The fulcrum (pivot point) is located 370 mm ahead of the cylinder. The wing has a cross-sectional shape of NACA0021, a span (s) of 120 mm and a chord length (c) of 30 mm. It is made from epoxy resin. This apparatus converts fluid energy into mechanical energy when the wing oscillates because of Karman vortices. A reflective tape is attached at the fixture for fixing the wing to the shaft so as to gauge the wing oscillation frequency with a laser beam digital tachometer installed behind of the wing. The vibration frequency at the wing oscillation amplitude (a) corresponding to each stroke (x = 1, 2, 3...12) of DE

was measured by adjusting an irradiation point of the laser beam (Fig. 15). The wing oscillating frequency was measured for 3 minutes and divided by the measurement time to obtain the DE frequency (f) that coincides with the wing frequency.

To identify the most effective position of the wing for producing electricity, the distance between the cylinder and the wing (L_{cw}) was varied from 50 to 210 mm by 10 mm for each U (0.30 to 0.70 m/s) and D (48, 60 and 76 mm). The generated power of this system may be calculated by using the frequency (f) and the stroke (x) of DE. The DEGs used in this experiment have the power generation performance shown in Fig. 11. Therefore, the electric power generation (P) of our system is expressed as the following equation.
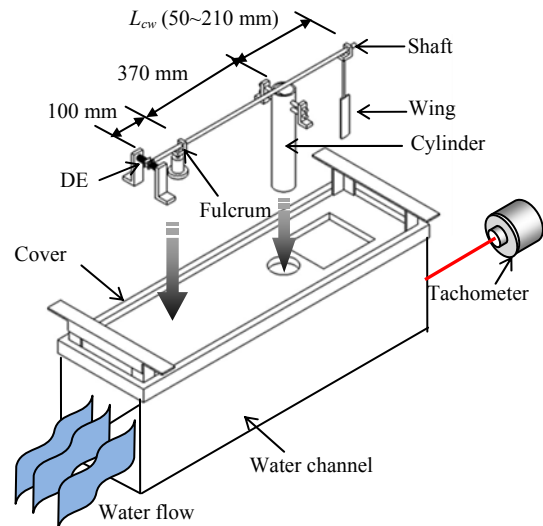
Fig. 14   Schematic drawing of the experimental apparatus.
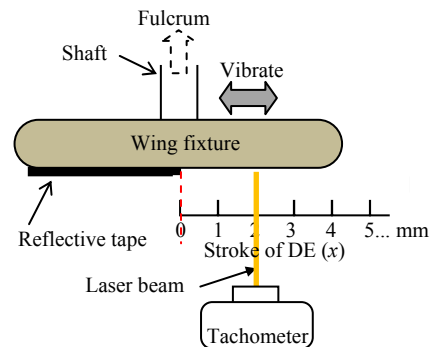
Fig. 15   Schematic view of the measuring system.

$$P = nHxf \qquad (7)$$

where n is the number of generation unit (2 units), and H is the power generation performance (1.254 mJ/mm) of DEG (Fig. 11d). However, $P = 0$ W when x is smaller than 1 mm, owing to the character of the DEG.

4. Results and Discussion

Fig. 16 shows the experimental results of the electric power generation (P) for cylinder diameters (D) of 48, 60 and 76 mm. For $D = 48$ mm, P is a maximum and its value is about 24.1 mW, when the non-dimensional distance between the cylinder and the wing (L_{cw}/D) is 3.5 and Re is $2.1{\times}10^4$, as shown in Fig. 16a. For $D = 60$ mm, P is a maximum and its value is about 31.0 mW, when L_{cw}/D is 2.8 and Re is $3.0{\times}10^4$, as shown in Fig. 16b. For $D = 76$ mm, P becomes maximum and its value is about 25.7 mW, when L_{cw}/D is 2.6 and Re is $4.2{\times}10^4$, as shown in Fig. 16c. We can say that only one peak mountain exists in each diagram about the electric power generation as shown in Fig. 16. Therefore, in this system, we have to choose the condition of this peak, i.e., Re and L_{cw}/D, to get the largest electric generation. We also should note that there is almost no electricity generation if the conditions are far from the peak in the results graph of this system. Vortices which drive the wing are not fully developed near the cylinder and become weak due to fluid viscosity far from the cylinder. It is noted that further computational analysis would be effective to find the best condition

about Re and L_{cw}/D to get highest value of the electric generation. Now, we consider a non-dimensional wing oscillation amplitude (a/D) and a reduced velocity (U_r) which is a non-dimensional velocity and defined as:

$$U_r = U/f_n D \qquad (8)$$

where f_n is the natural frequency of the system. f_n at each principal L_{cw} has been measured by averaging several free vibration tests and is shown in Table 1. Fig. 17 shows a/D as a function of U_r for $D = 60$ mm. From the results, a/D is found to become larger around $U_r = 5$. When a wing vibration frequency (f) corresponds to f_n, that is the resonant frequency, U_r can be written in the form.

$$U_r = U/f_n D \approx U/f_v D \qquad (9)$$

because Karman vortices drive the wing with the vortex shedding frequency (f_v). The third side of Eq. (9) is found to be the reciprocal of the St defined in Eq. (6). Therefore, $U_r = 1/St$ is obtained. Since St is experimentally found to be approximately equal to 0.2 in the range $500 < Re < 3.7{\times}10^5$ for circular cylinders [41], U_r becomes about 5 and a/D becomes a resonant amplitude.

As shown in Fig. 17, the maximum wing oscillation amplitude (a) is very small compared to the cylinder diameter (D). Because the projected area of the cylinder becomes larger than the total swept area of the wing trailing edge, the input power to this system is expressed as:
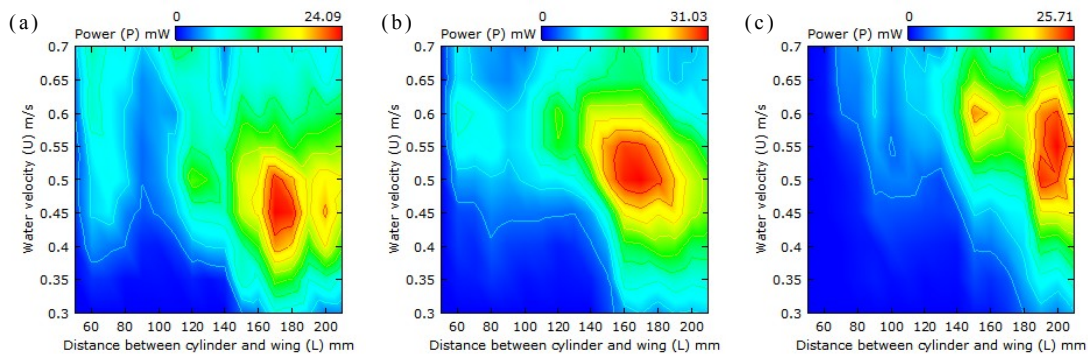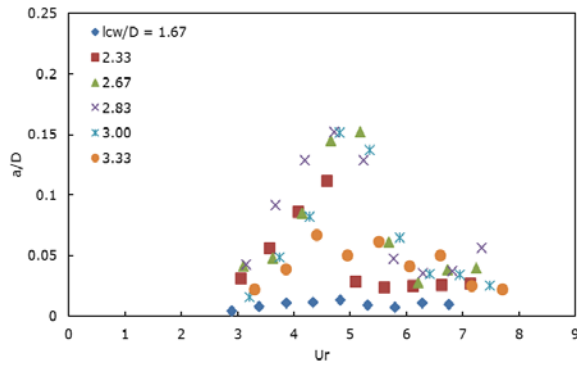
$$P_{in} = \rho A U^3 \qquad (10)$$

Fig. 16   The electric power generation (P) for cylinder diameters (D) of (a) 48 mm, (b) 60 mm and (c) 76 mm. The horizontal axis indicates the non-dimensional distance between the cylinder and the wing (L_{cw}/D). The vertical axis indicates Re.

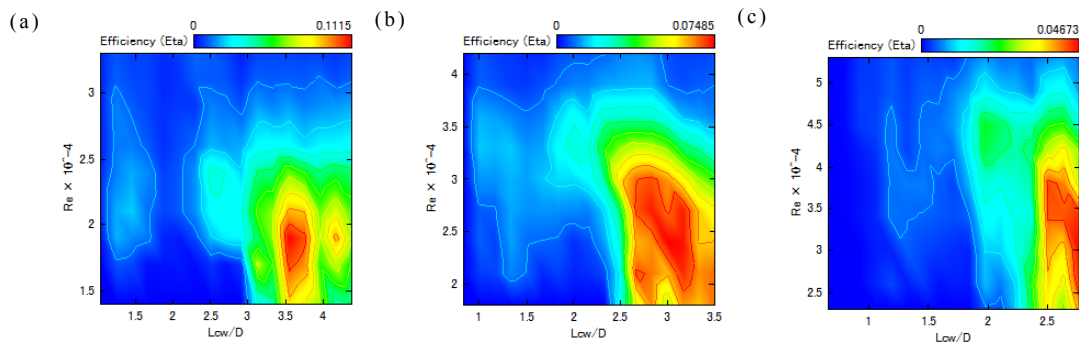**Table 1   Natural frequency (f_n) of the fabricated model.**

Distance between the cylinder and the wing (L_{cw}) mm	Natural frequency (f_n) Hz
100	1.73
140	1.64
160	1.61
170	1.59
180	1.59
200	1.52

Fig. 17   Non-dimensional wing oscillation amplitude (*a/D*) as a function of reduced velocity (*U_r*) for a cylinder diameter (*D*) of 60 mm.

where ρ is water density and A is the project area of the cylinder, the energy conversion ratio (η), i.e., the total efficiency, of this system is expressed as:

$$\eta = P/P_{in} = nHxf\big/\rho AU^3 \tag{11}$$

Fig. 18 shows the experimental results of the energy conversion ratio (η) for D of 48, 60 and 76 mm. For D = 48 mm, the energy conversion ratio (η) becomes maximum and its value is about 11.2%, when the

non-dimensional distance between the cylinder and the wing (L_{cw}/D) is 3.5 and Re is 1.9×10^4, as shown in Fig. 18a. For D = 60 mm, η becomes maximum and its value is about 7.5% when L_{cw}/D is 3.0 and Re is 2.4×10^4, as shown in Fig. 18b. For D = 76 mm, η becomes maximum and its value is about 4.7% when L_{cw}/D is 2.8 and Re is 3.0×10^4, as shown in Fig. 18c. Not surprisingly, the maximum power generation point of the diagram, i.e., the values of L_{cw}/D and Re, in Fig. 18 roughly correspond to that in Fig. 16.

In summary, the measured maximum for electric power generation (P) was about 31.0 mW when the cylinder diameter (D) is 60 mm, the non-dimensional distance between the cylinder and the wing (L_{cw}/D) is 2.8 and Re is 3.0×10^4. Under these conditions, the energy conversion ratio (η) was 6.9%, and the vortex shedding frequency (f_v) is found to be approximately 1.75 Hz by using U = 0.50 m/s, D = 60 mm and Eq. (6). As mentioned in the introduction, an electric power generation system using VIV and a conventional generator such as electromagnetic induction or the piezoelectric effect requires a high frequency (i.e. 60 Hz for a water flow [9, 10], 900 Hz for an air flow [11]) and drives with a low output energy compared to our proposed system using VIV and DEG. If Karman vortex street naturally existing in a wake of bridge piers is utilized as input power, η may be equivalent to about 66% because A shown in Eq. (11) can be considered as the smaller projecting

Fig. 18   The energy conversion ratio (η) for the cylinder diameters (*D*) of (a) 48 mm, (b) 60 mm and (c) 76 mm. The horizontal axis indicates the non-dimensional distance between the cylinder and the wing (*L_{cw}/D*). The vertical axis indicates *Re*.

area of a wing than a cylinder. The η of 66% is superior to the maximum energy conversion efficiency of 55% by wind power generation using DEG [28].
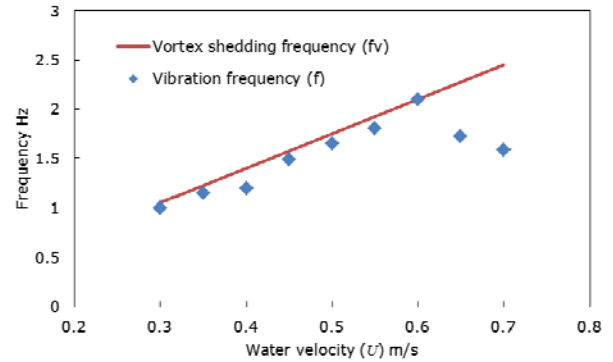
Fig. 19 shows the frequency of Karman vortex generation (f_v) and the vibration of the DEs (f) for $D =$ 60 mm and $L_{cw}/D = 2.8$. It is noted that the theoretical f_v corresponded well to the experimental results of f when Re is less than 3.6×10^4. This means that the driving force of the DEGs came from the pressure of the vortex. As Re becomes larger, a turbulent component in the wake of a cylinder becomes stronger. Therefore, we surmise that when Re is larger than 3.9×10^4, the strong turbulent component makes f smaller than the theoretical f_v.

Fig. 20 shows a histogram of the power generation (P) for a cylinder of diameter (D) 60 mm and the non-dimensional distance between the cylinder and the wing (L_{cw}/D) of 2.8. The components of P in this system were found not to have constant electric energy (E) per cycle (stretching and relaxing motion of DE). For an Re of 2.4×10^4, the wing and the DEGs oscillate at a frequency of about 1.2 Hz (Fig. 19) and P of about 14.8 mW is produced (Fig. 16b). In this vibration of the DE, E of 6.1 mJ per cycle accounts for approximately 60% of P and E of 7.6 mJ, 4.6 mJ account for about 25% and 15%, respectively. For Re = 3.0×10^4, the frequency of the DEGs (f) and P are approximately 1.7 Hz and 31.0 mW (Figs. 19 and 16b), respectively. E of 9.1 and 10.6 mJ per cycle account for about 80% of P and E of 7.6 mJ accounts for the rest of P. When Re becomes 3.6×10^4, the DEGs oscillate with f of about 2.1 Hz and produce P of about 20.4 mW (Figs. 19 and 16b). The components of P are dispersed from E of 1.5 mJ to E of 7.6 mJ with about 20%. The unstable wing oscillation for $Re = 3.6 \times 10^4$ is assumed to be caused by strong turbulence in the wake of the cylinder. Therefore, P for $Re = 3.6 \times 10^4$ became smaller than that for $Re = 3.0 \times 10^4$.

Based on the experimental results, the optimal conditions under which the maximum power

generation is obtained were explored. Electric energy generated by DEG per cycle becomes smaller if the wing is set near or far from the cylinder, because vortices for driving the wing are not fully developed near the cylinder and decay due to fluid viscosity far from the cylinder. Furthermore, the stroke and the frequencies of the DEGs decrease because of strong turbulence when the water velocity increases.

Electric power produced by scaling up the system may be estimated by understanding the dimensional factors. The experimental conditions in which the maximum power generation (P) of 31.0 mW is obtained are as follows: a cylinder diameter (D) of 60 mm; the distance between the cylinder and the wing

Fig. 19 The frequency of Karman vortex generation (f_v) and the vibration of the DEGs (f) for a cylinder diameter (D) of 60 mm and the non-dimensional distance between the cylinder and the wing (L_{cw}/D) of 2.8. The blue plots show the experimental results of f and red line shows the theoretical f_v from Eq. (6).
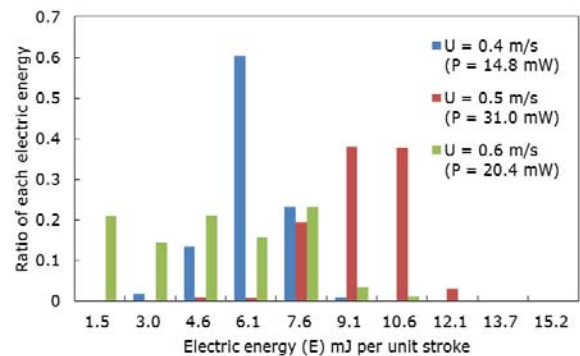
Fig. 20 Histogram of the power generation (P) for a cylinder diameter (D) of 60 mm, the non-dimensional distance between the cylinder and the wing (L_{cw}/D) of 2.8 and Re of 2.4×10^4, 3.0×10^4 and 3.6×10^4.

(L_{cw}) of 170 mm; a water velocity (U) of 0.5 m/s. The wing used in this study has a cross-sectional shape of NACA0021, a chord length (c) of 30 mm and a span length (s) of 120 mm. Under these conditions, the wing and the DEGs oscillate at a frequency of about 1.67 Hz (Fig. 19). Since the driving force (T), which gives a stroke to the DEGs, is obtained by the characteristics of the DEG (Fig. 11) and corresponds to the lift (L) acting on the wing in terms of the moment around the fulcrum, L is expressed as:

$$L = L_{df} / (L_{cw} + L_{fc})T \qquad (12)$$

where L_{df} is the distance between the DEGs and the fulcrum (100 mm) and L_{fc} is the distance between the fulcrum and the cylinder (370 mm). Moreover, L is non-dimensionalized by the dynamic pressure ($0.5\rho U^2$) and the wing area (cs) as the following equation.

$$C_L = L / 0.5\rho U^2 cs \qquad (13)$$

where C_L is the lift coefficient and ρ is the fluid density. The non-dimensionalized values based on the chord length (c) of this system in which the electric power generation becomes maximum are shown in Table 2.

Power generation (P) is estimated by varying the chord length (c) of the wing under the conditions shown in Table 2. First, systems must be geometrically similar, that is, a cylinder diameter of $D = 2c$, the distance between the cylinder and the wing of $L_{cw} = 5.67c$, the distance between the DEGs and the fulcrum of $L_{df} = 3.33c$, the distance between the fulcrum and the cylinder of $L_{fc} = 12.33c$, a wing span length of $s = 4c$. Second, since the similarities of Re and St cannot be simultaneously satisfied, we focused on St for kinematic similarity because periodic vibration induced by vortices is considered the most important parameter in this system. As matching of the vortex shedding frequency (f_v) and a natural frequency (f_n) is very important to obtain high power generation, the water velocity (U) is set to be $U = f_n D/St = 2cf_n/0.2$ from Eq. (6). Consequently, the wing vibrates at a frequency of $f = f_v = f_n$ in accordance with Karman vortices periodically generated at a frequency of $f_v = f_n$. It is noted that St is approximately 0.2 in $500 < Re < 3.7 \times 10^5$ in circular cylinders, which means that the wing chord length (c) must satisfy $25v < c^2 f_n < 1.85 \times 10^4 v$ from Eq. (5). Finally, using Eqs. (12) and (13) the driving force (T) can be obtained.

Fig. 21 shows driving forces (T) and water velocities (U) as a function of the wing chord length (c) when the natural frequencies (f_n) of scaled up systems are assumed to be 0.50, 1.00, 1.67 and 2.00 Hz. Re exceeds a critical Re of 3.7×10^5 around approximately $T = 500$ N for any frequency, while c at which Re reaches the critical Re varies for each frequency. c becomes about 190, 135, 105 and 95 mm for $f = 0.50$, 1.00, 1.67 and 2.00 Hz, respectively. Diaphragm-type DEGs with a DE diameter of 80 mm have the generation performance of 0.405 N/mm and 1.254 mJ/mm per cycle as shown in Figs. 11c and 11d. If the maximum allowable stroke of the DEGs is 12 mm, this system is capable of being equipped with approximately 100 units of the DEG and generating electric energy of about 1.5 J per cycle. The scaled-up system equipped with 100 units of the DEG can be expected to generate electric power of approximately 3 W with a wing chord length of 95 mm and a water velocity of 1.9 m/s for a frequency of 2.00 Hz.

Electric energy can be harvested from a small ocean wave with a wave power generation system using

Table 2　Non-dimensional parameters of the device.

D/c	L_{cw}/c	L_{df}/c	L_{fc}/c	s/c	Re	St	C_L
2	5.67	3.33	12.33	4	1.5×10^4	0.2	2.82
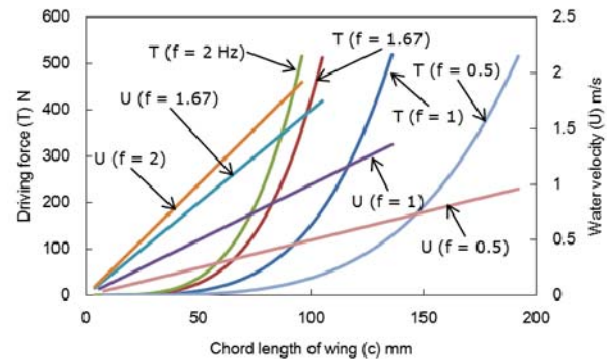
Fig. 21　Driving force (T) and water velocity (U) as a function of chord length of wing (c).

DEG, which means that the generation system can supply energy to fisheries industries near shore such as aquaculture, fixed-net fishing, etc. In these industries, utilization of various sensor systems and security systems has been under consideration and power-saving and efficiency are required.

We can also expect that our proposed system is capable of supplying power to street lamps on a bridge and remote sensing devices for fatigue cracks of a bridge using Karman vortices in the wake of the bridge piers. Furthermore, by using Karman vortices in the wake of riser pipes used in ocean development, our system can supply energy to remote sensors for those positions and fatigue crack.

5. Conclusions

DEG driven by Karman vortices in water flow was proposed for small scale hydropower systems. From the experimental results, we obtained the following conclusions:

(1) An electric generator using DEs with 80 mm diameter driven by Karman vortices in water flow was successfully demonstrated.

(2) We have to carefully select the diameter of the cylinder and the distance between the cylinder and the wing corresponding to the fluid velocity in order to get high efficiency of this electric generation system.

(3) The maximum energy efficiency is about 11.2% in this system.

(4) The maximum average electric power of approximately 31.0 mW is obtained with a generation efficiency of about 6.9%.

(5) An electric energy of approximately 1.5 J per cycle of DEGs can be expected to be generated by scaling up this system, which is capable of being equipped with up to about 100 units of the DEG.

Acknowledgments

References

[1] REN21. 2011. Renewables 2011 Global Status Report, Paris, REN21 Secretariat, 2011.

[2] Miyazaki, T., and Osawa, H. 2007. Search Report of Wave Power Devices. Presented at The 2007 Spring Conference of the Japan Society of Naval Architects and Ocean Engineers, No.4, 43-6.

[3] Ashida, K., Ichiki, M., Tanaka, M., and Kitahara, T. 2000. "Power Generation Using Piezo Element: Energy Conversion Efficiency of Piezo Element." In *Proc. of JAME Annual Meeting*, 139-40.

[4] Chiba, S. 2014. *Dielectric Elastomers, Soft Actuators (Materials, Modeling, Applications, and Future Perspectives)*, Chapter 13, edited by Asaka, K., and Okuzaki, H, 183-95. ISBN:978-4-431-54766-2. DOI: 10.1007/978-4-431-54767-9.

[5] Yuan, X., Changgeng, S., Yan, G., and Zhenghong, Z. 2016. "Application Review of Dielectric Electroactive Polymers (DEAPs) and Piezoelectric Materials for vibration Energy Harvesting." *Journal of Physics: Conference Series* 744: 12-77.

[6] Waki, M., and Chiba, S. 2016. "Elastomer Transducers." *Advances in Science and Technology (Trans Tech Publications)* 97: 61-74. ISSN: 1662-0356.

[7] Allen, J. J., and Smits, A. J. 2001. "Energy Harvesting Ell." *Journal of Fluids & Structures* 15 (3-4): 629-40.

[8] Zhu, D., Beeby, S., Tudor, J., White, N., and Harris, N. 2010. "A Novel Miniature Wing Generator for Wireless Sensing Applications." In *Proc. of the 9th IEEE Conference on Sensors 2010*, Waikoloa, Hawaii, USA.

[9] Akaydin, H. D., Elvin, N., and Andreopoulos, Y. 2010. "Wake of a Cylinder: A Paradigm for Energy Harvesting with Piezoelectric Materials." *Experiments in Fluids* 49: 291-304.

[10] Wang, D. A., Chiu, C. Y., and Pham, H. T. 2012. "Electromagnetic Energy Harvesting from Vibrations Induced by Karman Vortex Street." *Mechatronics* 22: 746-56.

[11] Wang, D. A., Chao, C. W., and Chen, J. H. 2012. "A Miniature Hydro-energy Generator Based on Pressure Fluctuation in Karman Vortex Street." *Journal of Intelligent Material Systems and Structures* 24 (5): 612-26.

[12] Nguyen, H. D. T., Pham, H. T., and Wang, D. A. 2013. "A Miniature Pneumatic Energy Generator Using Karman Vortex Street." *J. Wing Eng. Ind. Aerodyn.* 116: 40-8.

[13] Demori, M., Ferrari, M., Ferrari, V., Farise, S., and

Poesio, P. 2014. "Energy Harvesting from Von Karman Vortices in Airflow for Autonomous Sensors." *Procedia Engineering* 87: 775-8.

[14] Pelrine, R., and Chiba, S. 1992. "Review of Artificial Muscle Approaches." (Invited) In *Proc. of Third International Symposium on Micromachine and Human Science*, Nagoya, Japan, 1-9.

[15] Kornbluh, R. D., Heydt, R., and Pei, Q. 1999. "High-Field Electrostriction of Elastrometric Polymer Dielectrics for Actuation." *Smart Structures & Materials Electroactive Polymer Actuators & Devices*.

[16] Pelrine, R., Kornblue, R., Joseph, J., Pei, Q., and Chiba, S. 2000. "High-field Deformation of Elastomeric Dielectrics for Actuators." *Material Science and Engineering* C11: 89-100.

[17] Chiba, S. 2002. "MEMS and NEMS Applications of Dielectric Elastomer and Future Trends." *Electronic Packaging Technology* 18 (1): 32-8.

[18] Chiba, S., Waki, M., Kornbluh, R., and Pelrine, R. 2011. "Current Status and Future Prospects of Power Generators Using Dielectric Elastomers." *Smart Materials and Structures* 20 (12): 11516-43.

[19] Koh, S. J. A., Zhao, X., and Suo, Z. 2009. "Maximal Energy That Can Be Converted by a Dielectric Elastomer Generator." *Applied Physics Letters* 94 (26): 262902-3.

[20] Huang, J., Shian, S., Suo, Z., and Clarke, D. 2013. "Maximizing the Energy Density of Dielectric Elastomer Generators Using Equi-Biaxial Loading." *Advanced Functional Materials* 23: 5056-61.

[21] Lin, G., Chen, M., and Song, D. 2009. In *Proc. of the International Conference on Energy and Environment Technology* (ICEET '09), 782-6.

[22] Brouchu, P. A., Li, H., Niu, X., and Pei, Q. 2010. "Factors Influencing the Performance of Dielectric Elastomer Energy Harvesters." In *Proc. SPIE,* 7642, 7622J.

[23] Vertechy, R., Papini Rosati, G. P., and Fontana, M. 2015. "Reduced Model and Application of Inflating Circular Diaphragm Dielectric Elastomer Generators for Wave Energy Harvesting." *Journal of Vibration and Acoustics, Transactions of the ASME* 137: 11-6.

[24] Bortot, E., and Gei, M. 2015. "Harvesting Energy with Load-Driven Dielectric Elastomer Annular Membranes Deforming Out-of-Plane." *Extreme Mech. Lett.* 5: 62-73.

[25] Moretti, G., Fontana, M., and Vertechy, R. 2015. "Parallelogram-Shaped Dielectric Elastomer Generators: Analytical Model and Experimental Validation." *Journal of Intelligent Material Systems and Structures* 26 (6): 740-51.

[26] Brochu, P., Yuan, W., Zhang, H., and Pei, Q. 2009. "Dielectric Elastomers for Direct Wind-to-Electricity Power Generation." In *Proc. of ASME 2009 Conference on Smart Materials, Adaptive Structures and Intelligent System*.

[27] Zhou, J., Jiang, L., and Khayat, R. 2016. "Dynamic Analysis of a Tunable Viscoelastic Dielectric Elastomer Oscillator under External Excitation." *Smart Materials and Structures* 25 (2): 025005.

[28] McKay, T., O'Brien, B., Calius, E., and Anderson, I. 2011. "Soft Generators Using Dielectric Elastomers." *Applied Physics Letters* 98 (14): 142903, 1-3.

[29] Anderson, I., Gisby, T., McKay, T., O'Brien1, B., and Calius, E. 2012. "Multi-functional Dielectric Elastomer Artificial Muscles for Soft and Smart Machines." *J. Appl. Phys.* 112 (4): 041101.

[30] Van Kessel, R., Wattez, A., and Bauer, P. 2015. "Analyses and Comparison of an Energy Harvesting System for Dielectric Elastomer Generators Using a Passive Harvesting Concept: The Voltage-clamped Multi-phase System." In *SPIE Smart Structures and Materials+ Nondestructive Evaluation and Health Monitoring*, International Society for Optics and Photonics, 943006.

[31] Ashida, K., Ichiki, M., Tanaka, M., and Kitahara, T. 2000. "Power Generation Using Piezo Element: Energy Conversion Efficiency of Piezo Element." In *Proc. of JAME annual meeting*, 139-40.

[32] Chiba, S., Waki, M., Kornbluh, R., and Pelrine, R. 2008. "Innovative Power Generators for Energy Harvesting Using Electroactive Polymer Artificial Muscles." In *Proc. SPIE 6927, Electroactive Polymer Actuators and Devices (EAPAD)*, 692715, 1-9.

[33] Zurkinden, A., Campanile, F., and Martinelli, L. 2007. "Wave Energy Converter through Piezoelectric Polymers." In *Proc. COMSOL User Conference 2007*, Grenoble, France.

[34] Jean-Mistral, C., Basrour, S., and Chaillout, J. 2010. "Comparison of Electroactive Polymer for Energy Scavenging Applications." *Smart Materials & Structures* 19 (19): 085012.

[35] Chiba, S., Waki, M., Wada, T., Hirakawa, Y., Matsuda, K., and Ikoma, T. 2013. "Consistent Ocean Wave Energy Harvesting Using Electroactive (Dielectric Elastomer) Artificial Muscle Generators." *Applied Energy* 104: 497-502, ISSN: 0306-2619.

[36] Chiba, S., Waki, M., Kornbluh, R., and Pelrine, R. 2010. "Novel Electric Generator Using Electro Polymer Artificial Muscles." In *Proc., 18th World Hydrogen Conference 2010, Hydrogen Production Technologies – Part 2*, Essen, Germany, 78-3, 23-30, ISBN: 978-3-89336-653-8.

[37] Chiba, S., Waki, M., Masuda, K., Ikoma, T., Osawa, H., and Suwa, Y. 2012. *Innovative Power Generation System for Harvesting Wave Energy, Design for Innovative*

Value towards a Sustainable Society. Netherlands: Springer, 1002-7, ISBN 978-94-007-3010-6.

[38] Moretti, G., Forehand, D., Vertechy, R., Fontana, M., and Ingram, D. 2014. "Modeling of an Oscillating Wave Surge Converter with Dielectric Elastomer Power Take-off." In *Proceedings of the International Conference on Offshore Mechanics and Arctic Engineering—OMAE*, 9A.

[39] Vertechy, R., Fontana, M., Rosati Papini, G. P., and Forehand, D. 2014. "In-tank Tests of a Dielectric

Elastomer Generator for Wave Energy Harvesting." In *Proceedings of SPIE—The International Society for Optical Engineering*, 9056.

[40] Chiba, S., et al. 2017. "Simple and Robust Direct Drive Water Power Generation System Using Dielectric Elastomers." *Journal of Material Science and Engineering* B7 (1-2): 39-47. DOI: 10.17265/2161-6213/2017.1-2.005.

[41] The Japan Society of Fluid Mechanics. 1998. *Handbook of Hydrodynamics*, 2nd ed., Maruzen.